Substituted 2-nitrobenzyltrichloroacetate esters for photodirected oligonucleotide detritylation in solid films†

Pawel J. Serafinowski*[a] and Peter B. Garland[b]

Received 23rd April 2008, Accepted 3rd July 2008
First published as an Advance Article on the web 23rd July 2008
DOI: 10.1039/b806902f

Oligonucleotide microarray fabrication by chemical synthesis using photoacid generators in solid films could have advantages over existing methods, but has not matched the accuracy of conventional synthesis where detritylation is performed with acid solutions. To address this problem, we explored the kinetics and equilibria of nucleoside detritylation in solid films, using trichloroacetic acid (TCA) generated by photolysis from its esters with substituted 2-nitrobenzyl alcohols. We synthesised 25 such esters, all α-phenyl substituted, and assessed their potential as solid film photoacid generators. They included sets with (i) mono- or dimethoxy-, (ii) 5-halo-, (iii) alkyl- or aryl-substituted 5-amino-, or (iv) 5-aryl-substituents in the 2-nitro- or 2,6-dinitrobenzyl ring. Absorption maxima of their UV spectra ranged from 230 to 410 nm, with quantum yields at 365 nm from < 0.01 to nearly 1.0. The esters formed optically clear solid films on glass slides without added polymer. Kinetics of intrafilm photoacid generation, proton activity changes and detritylation were measured *in situ.* The most effective esters for light sensitivity and detritylation were 5-chloro-, 5-bromo-, 4,5-dimethoxy-, and 4- or 5-aryl-substituted 2,6-dinitrobenzyl esters. Photoacid-induced increases in proton activity and detritylation were severely inhibited by polymers containing electronegative heteroatoms, but not by polymers lacking them. In solid films, intrafilm detritylation with photogenerated TCA was fast, but stopped at an equilibrium well short of completion. Both experiment and theory emphasise the inadequacy of attempting to force detritylation with high intrafilm acid activity.

Introduction

The trityl group is widely used for acid-labile protection of hydroxyl groups during organic syntheses.[1] It was introduced as the dimethoxytrityl form (DMT²) for protection of the 5′-OH group of nucleoside monomers in oligonucleotide synthesis,[3–5] normally carried out on a solid phase of glass or plastic beads. Removal of the DMT group prior to each successive round of oligonucleotide chain lengthening is achieved with acid: it is a reversible reaction and goes to completion if released DMT^+ is removed by the fluid phase. Detritylation can also approach completion if strong acids are used, but their ability to cause depurination is unacceptable. High synthetic yields and oligonucleotide purity require high deprotection yields, ideally 100%. This requirement is critical when oligonucleotides are synthesised *in situ* at an array surface.

Photosensitive protecting groups were introduced in place of acid-removable DMT groups for fabrication of oligonucleotide arrays on planar glass surfaces using patterned illumination.[6] These had disadvantages of high cost and low light sensitivity, but nevertheless successfully launched the use of photolithography in this field.

Photolithographically generated acid-patterns must not be degraded by subsequent diffusion if the acid is photogenerated in solution. This requirement can be met by a system of microwells[7] and microfluidics.[8] Such options for DMT^+ removal are unavailable if photoacid generation is within a diffusion-restricting solid film applied to the array surface.[9] Although the detritylation equilibrium position can be shifted further towards completion by use of stronger photoacids, conflict occurs between the needs for high stepwise yield and absent depurination. Stepwise yields in these circumstances have not exceeded 94% in the absence of unacceptable depurination,[9] giving overall yields of $\leq 0.94^N$ for an N-mer, or ≤ 29% for a 20-mer. Such yields have attracted critical comment.[10]

Nevertheless the use of solid films of photoacid generators for oligonucleotide array fabrication offers potential advantages of very high density of array elements and reduced costs. We had demonstrated[11] that TCA photogenerated from its substituted 2-nitrobenzyl ester in solution could achieve >99% stepwise yields for oligonucleotide synthesis on glass beads, and decided to explore the possibility of achieving similar yields when TCA is generated in a solid film.

Our approach as described here was two-fold. We synthesised and characterised a wider range of PAGs based on TCA esters of substituted 2-nitrobenzyl alcohols. Their photochemical properties can be tailored by changes of substituents.[12] Other advantages include the ease with which they form solid films, and the absence of chemically aggressive photoreaction intermediates. In parallel we developed UV–vis spectrophotometric methods for directly measuring within solid films the kinetics of photo-induced TCA generation, acidification and detritylation. We were then able to characterise some main factors affecting the equilibrium position of detritylation within a solid film.

[a]*Cancer Research UK Centre for Cancer Therapeutics, Sutton, Surrey, UK SM2 5NG. E-mail: pawel.serafinowski@icr.ac.uk*
[b]*Section of Molecular Carcinogenesis, The Institute of Cancer Research, Sutton, Surrey, UK SM2 5NG. E-mail: peter@garland.org.uk*
† Electronic supplementary information (ESI) available: Experimental. See DOI: 10.1039/b806902f

Results and discussion

Strategy for synthesis of esters

Fig. 1 shows the general structure for the 25 photosensitive TCA esters of substituted 2-nitrobenzyl alcohol that we have synthesised. In 4 other related PAGs the acid was *p*-toluenesulfonic, acetic, HCl or HBr.

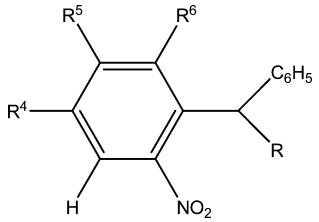

Fig. 1 Photosensitive esters and precursors. R = $OCOCCl_3$ or R = OH. Table 1 and ESI describe R^4–R^6.† In all cases, R^2 is NO_2 and R^3 is H. The α-phenyl substituent was present in all esters listed in Table 1 below, except for **26–29**.

The TCA esters were all α-phenyl substituted to improve quantum yields.[12] They fall into four families defined by substituents of the 2-nitro or 2,6-dinitrobenzyl ring. As shown in Table 1, the families are (i) methoxy-substituted (**1–4**), (ii) halo-substituted (**5–10**), (iii) alkylamino, arylamino, or phenylazo-substituted (**11–19**) and (iv) aryl-substituted (**20–25**). Their general synthetic pathway started with 5-bromo-, 5-iodo- 5-chloro- or 5-fluoro-2-nitro-benzylaldehyde or their 2,6-dinitro versions, which are either available commercially or made as described in the ESI.†

Introduction of the α-phenyl group was achieved by condensation of the aldehydes with phenyl magnesium bromide. Various benzyl ring substitutions were explored as a means of enhancing quantum yields and light absorption properties. A second nitro-group at the 6-position enhances quantum yield.[13,14] 5-Halo-substituted precursors were used in further synthetic transformations to introduce amino, aryl and phenylazo groups.

We anticipated that these conjugation-extending substituents would usefully increase extinction coefficients and shift absorption maxima to higher wavelengths. We also prepared two 2,6-dinitrobenzyl esters with 4-aryl substitution (**24**, **28**). The precursors (Fig. 1, R = OH) were finally converted into the corresponding trichloroacetate esters (Fig. 1, R = $OCOCCl_3$) by reaction with trichloroacetic anhydride.

Photochemical properties in solution

The structure, absorption spectra, and quantum yields of trichloroacetate esters **1–25** in dilute solution (10–50 μM) in DCM at ambient temperatures are summarised in Table 1. In all cases photolysis, as measured by time dependent changes in the UV and near visible absorption spectra during exposure to 365 nm light, proceeded as a first order reaction with a rate constant dependent on illumination intensity.

Compounds **1** and **2** are both 4,5-dimethoxy substituted 2-nitrobenzyl esters: **2** has a 6-nitro substitution.[15] They have reasonable extinction coefficients and quantum yields at 365 nm. The 5-halo-substituted esters **5–10** have their major absorption peaks well below 365 nm, but higher quantum yields partially compensated for lowered light sensitivity at 365 nm.

Substituted amino groups at the 5-position of the 2-nitrobenzyl ring gave large increases of height and position of the main absorption peak (esters **11–19**). They could be photolysed at 365 or 405 nm to their nitroso-photoproducts.

The 5-phenylazo substituted ester **19** had a low absorption shoulder extending to nearly 500 nm. On illumination at 365 nm the main peak at 335 nm fell by 40% within a few seconds without change in its position or shape. The quantum yield for this process was 0.3, and was probably due to *trans–cis* isomerism at the diazo double bond.[16] A higher absorption with a maximum at 365 nm and anticipated to be typical of the expected photoproduct, appeared on prolonged illumination, with a quantum yield of 0.02.

Compounds **20–25** possessed an additional aryl group. Photochemical properties depended strongly on substituents of both rings (Table 1). Because the bases of oligonucleotides can be directly damaged by UV light <310 nm, preferred PAGs have high extinction coefficients at longer wavelengths such as 365 nm or 405 nm. However, substitutions that increased absorption at higher wavelengths often lowered the quantum yields, and *vice versa*. Esters **2**, **15**, **16** and **21–24** were the most promising at 365 nm.

We also synthesised four esters of other acids. The 4,5-dimethoxy-2-nitrobenzyl tosylate **26** was stable and has already been used as a PAG.[14] Our attempts to make α-phenyl or α-methyl substituted versions failed because of spontaneous decay of the products: the former evolved to 4,5-dimethoxy-2-nitrosobenzophenone and the latter to a cyclic product, 5,6-dimethoxy-3-methyl-benzo[*c*]isoxazol-1(3*H*)-olate (ESI†). Instability of 2,6-dinitrobenzyl-*p*-toluenesulfonate has been described previously.[14] The 2,6-dinitrobenzyl chloride (**27**), bromide (**28**), and acetate (**29**), like the TCA esters in Table 1, are solids that can be stored in the dark at −20 °C for many months.

2,6-Dinitroesters: which nitro group becomes nitroso?

This question arises for unsymmetrical esters. We answered it by characterisation of the nitroso-photoproducts of some relevant esters and showed that the 2-nitro group was the one converted to a nitroso-group (ESI†).

Photochemical properties in solid films

Solution studies were used to identify potentially useful PAGs. Most of the esters listed in Table 1 formed optically clear films when their 2% (w/v) solutions in DCM were allowed to spread and dry on a flat glass surface. The exceptions were solutions of the 4- or 5-aryl-substituted esters **20–25**, which tended to round up rather than spread, unless mechanically assisted or in solution with a polymer. The ester films were not as hard as films of polymers such as PMMA or PS. Esters **8–10** formed the softest films.

The ester films, although thin, have absorption bands in the 300–420 nm region, allowing measurement of their photolysis, a reaction that, as in solution, followed first order kinetics. No significant primary photolytic reactions other than release of the acid and an equimolar amount of nitroso-photoproduct have been described. The nitroso-photoproducts have distinctive absorption spectra in the near UV or higher wavelengths, with maxima at higher wavelengths than the parent esters. Their absorption was used to calculate the parallel release of photoacid.

Table 1 Photochemical properties of substituted 2-nitrobenzyl esters in solution. Substituents R^4–R^6 are positioned as in Fig. 1. The esterifying acids were trichloroacetic for **1–25**, *p*-toluenesulfonic for **26** and acetic for **29**. Also included are substituted 2-nitrobenzyl halides **27** and **28**, which on photolysis yield HCl and HBr respectively. Esters **1–25** were α-phenyl substituted

	Atom or group at:				ε_{mM}/mM^{-1} cm^{-1} at:			
Ester[a]	R^4	R^5	R^6	λ_{max}/nm	λ_{max}	365 nm	405 nm	Φ^b
1[11]	OCH_3	OCH_3	H	345	5.3	3.5	<0.1	0.1–0.2
2[11]	OCH_3	OCH_3	NO_2	323	4.1	2.0	<0.1	0.4
3	OCH_3	H	H	329	4.1	nd	<0.1	nd
4	OCH_3	H	NO_2	314	3.2	0.84	<0.1	0.3
5	H	F	H	232	15.6	0.4	<0.1	0.1
6	H	Cl	H	270	6.2	0.32	<0.1	0.2
7	H	Cl	NO_2	256	7.5	0.23	<0.1	0.6–0.9
8	H	Br	H	276	6.6	0.31	<0.1	0.1
9	H	Br	NO_2	255	8.9	0.43	<0.1	0.3
10	H	I	H	296	6.5	0.7	0.22	0.3
11	H	$(Me)_2N$	NO_2	376	11.0	10.4	6.9	<0.01
12	H	$(Et_2)N$	NO_2	379	12.0	10.1	8.1	<0.01
13	H	Morpholin-1-yl	NO_2	361	7.6	7.2	3.1	0.08
14	H	Pyrrolidin-1-yl	H	403	22.7	14.6	22.5	<0.02
15	H	Pyrrolidin-1-yl	NO_2	380	14.6	12.8	8.2	0.10
16	H	Piperidin-1-yl	NO_2	380	13.1	12.1	5.7	0.08
17	H	*p*-Methoxyphenyl-amino	NO_2	370	8,2	8.1	5.5	<0.01
18	H	Phenylamino	NO_2	370	6.6	6.6	3.7	0.05
19	H	Phenylazo	H	335	24.0	15.0	1.0.	0.02[c]
				454	1.0	n.a	n.a	0.3[c]
20	H	*p*-$(Me)_2N$-phenyl	NO_2	410	7.1	5.0	6.9	0.01
21	H	Phenyl	NO_2	280	7.6	0.7	<0.1	0.5–0.6
22	H	4-Methoxyphenyl	NO_2	324	4.4	3.0	0.5	0.3
23	H	3,4-Dimethoxyphenyl	NO_2	347	4.8	4.1	1.2	0.1
24	4-Methoxyphenyl	H	NO_2	267	2.6	0.35	<0.1	0.8
25	H	5-Ethoxynaphthyl	NO_2	334	4.1	2.3	1.0	<0.01
26	OCH_3	OCH_3 (*tosylate ester*)	H	347	8.5	6.5	0.42	0.02
27[d]	Br	H (*benzyl chloride*)	NO_2	317	6.6	0.45	<0.1	0.4
28	4-Methoxyphenyl	H (*benzyl bromide*)	NO_2	298	2.2	2.2	<0.1	0.3
29[d]	Br	H (*acetate ester*)	NO_2	247	7.0	0.26	<0.1	<0.01

Notes: Spectral and photochemical values are for solutions in dichloromethane at 20–25 °C. [a] **1** and **2** were referred to previously[11] as esters A and D respectively. Substituted 2-nitrobenzyl halides **27** and **28** are photoacid generators of inorganic acids. [b] Quantum yields Φ for photolysis at 365 nm based on appearance of the absorption band of the substituted 2-nitrosobenzophenones. The values are the mean of at least 3 observations, which varied by ≤20%. [c] The entry for **19** describes both the main peak (335 nm) and the long wavelength shoulder (445 nm). The higher quantum yield is assumed to be for *cis–trans* isomerism, and the lower value for formation of the nitroso-photoproduct. [d] Use of 2-nitrobenzylhalides to generate hydrohaloacids has been previously proposed by others.[17] Abbreviation "n.a." is for "not applicable", "nd" for "not determined".

Acid-induced increases of intrafilm proton activity were followed at 640 nm by inclusion of a pH indicator[18] (brilliant green or BG, pK_a in aqueous solution *ca.* 0.7). To avoid possible complexities arising from restriction of DMT-nucleotide to a thin layer attached to the underlying glass surface, we used DMT-T incorporated in the film as a simple target for detritylation. The DMT^+ carbocation was detected at 510 nm, red-shifted from the solution maximum[3] at 505 nm.

Because of slight peak broadening and red shifts of *ca.* 5 nm in the solid state, we did not have precise values for extinction coefficients for the compounds measured in solid films. So we used the solution values to calculate approximate quantum yields in films: in general they were the same or slightly higher than in solution.

An example of spectra before and after photolysis for a film of **1** containing DMT-T and BG is given in Fig. 2. The absorption changes due to photolysis of the ester (appearance of a shoulder at *ca.* 400 nm due to the nitrosobenzophenone), increased intrafilm proton activity (fall of the BG peak at 640 nm) and the resulting detritylation of DMT-T (emergence of the DMT^+ peak at 510 nm) are all apparent. Replacement of ester **1** with **2** resulted in a 90% fall of the BG peak and *ca.* 80% conversion of DMT-T to DMT^+.

When tested in solid films, photolysis of the 5-alkylamino substituted esters **15** or **16** failed to increase intrafilm proton activity to levels detected by BG, nor was DMT^+ production observed. Presumably the heterocyclic nitrogen-containing substituents were sufficiently basic to bind protons. By contrast **2**, **7** and **21–24** were highly effective, 25% photolysis causing almost complete flattening of the BG peak at 640 nm, and extensive detritylation. Ester **24** was also effective with 405 nm as the photolysing wavelength.

Despite the several-fold lower extinction coefficient of **7** at 365 nm when compared to **2**, it was no less effective in detritylation of DMT-T on illumination. It also had the advantage of negligible interference with DMT^+ detection at 510 nm from its nitroso-photoproduct. Faced with several effective esters, it was necessary to elect one that would allow us to carry out a wide range of further experiments, described below, that were primarily concerned with the performance of TCA in relation to detritylation, rather than the PAG itself. We chose ester **2**.

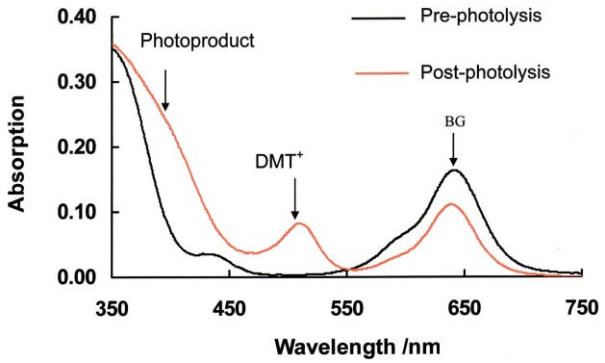

Fig. 2 Simultaneous measurement of intrafilm photoacid generation, photoacid activity and detritylation. Absorption spectra before and after illumination of a film of **1** containing DMT-T and BG. The casting solution contained 40 mM ester **1**, 0.74 mM BG and 0.7 mM DMT-T in DCM. Photolysis was at 365 nm (390 mJ cm^{-2}). Under these conditions detritylation was *ca.* 40% complete, and *ca.* 80% if **2** replaced **1**.

Effects of including polymers on intrafilm acidification and detritylation. Others have used PMMA[9] as a film-forming matrix. If an experiment as in Fig. 2 was repeated with PMMA present in the film casting solution at a 1 : 1 or 2 : 1 ratio (w/w) to either **1** or **2**, then although production of TCA as measured by accumulation of the nitroso-photoproduct was unaffected, very little rise of intrafilm proton activity (640 nm) or detritylation (510 nm) was seen.

We explored the ability of PMMA to prevent photogenerated TCA from increasing intrafilm acidity and effecting detritylation by carrying out what in effect were intrafilm titrations of proton activity in response to increasing photoacid concentration. Fig. 3 shows results using a pair of incorporated pH indicators, BG and

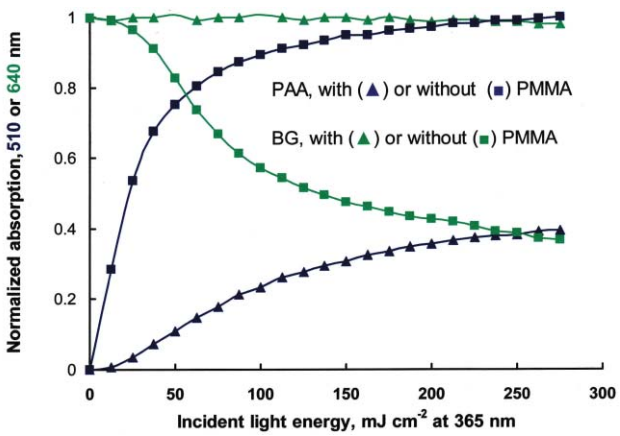

Fig. 3 Effects of PMMA on intrafilm pH changes in response to photogeneration of TCA. The surface area densities for ester **2**, BG (pK_a = 0.7) and PAA (pK_a = 2.3) in the films were 105, 2, and 1.2 nmol cm^{-2} respectively. Illumination at 365 nm (10 mW cm^{-2}) was continuous, *via* a dichroic filter. Absorption spectra from 420 to 750 nm were periodically recorded during photolysis. Absorption values for the protonated PAA (510 nm) and non-protonated BG (640 nm) at each time interval were used to construct the figure. The BG values were normalised to their pre-photolysis values, and the PAA values to the maximum observed in the absence of PMMA. The ratio of PMMA to **2** in the films was either zero or 2 : 1 (w/w).

PAA (4-phenylazoaniline: pK_a value ≈ 2.3 in aqueous media).[18] The inclusion of PMMA converted intra-film TCA into a weaker acid, able to protonate PAA but hardly able to protonate BG at all. This effect of PMMA on the apparent pK_a value of TCA can also be demonstrated in DCM solution simply by titration of the acid responses of BG and PAA to TCA with or without the polymer.

We concluded that the effect of PMMA on the strength of photogenerated TCA was responsible for inhibition of detritylation. Carboxylic acids readily form homodimers by hydrogen bonding,[19] and the acidic hydrogen of monomeric TCA could bond with electronegative atoms of different molecules such as PMMA, in which case a polymer deficient in electronegative heteroatoms would have little if any effect on the strength of TCA. This prediction was fulfilled when PSMS replaced PMMA (Fig. 4).

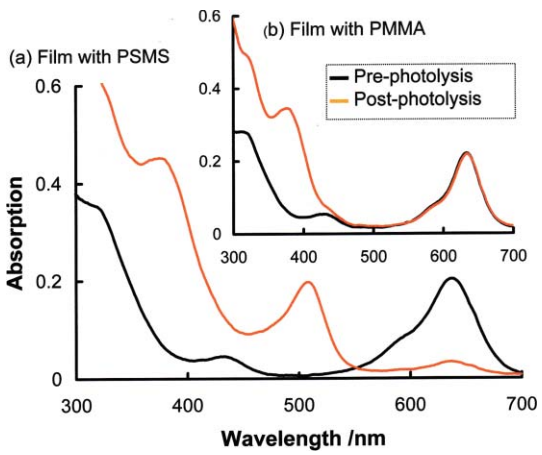

Fig. 4 Effect of PMMA or PSMS on acid strength in films. Panel (a) absorption spectra before and after photolysis (1.1 J cm^{-2} at 365 nm) of a film cast from 2% PSMS, 0.2 mM BG, 6.3 mM ester **2** and 0.2 mM DMT-T. Panel (b) as (a) but PSMS replaced by PMMA.

To provide further evidence for weakening of photogenerated TCA by hydrogen bonding to electronegative heteroatoms, we examined a range of film-forming polymers with or without such atoms. The number of possibilities is large: we considered *ca.* 3000.[20] In addition to PMMA and PSMS already tested (Fig. 3), we selected a further 41 that were easily dissolved in DCM, formed suitable films, and covered a range of compositions.

Of the 43 polymers tested for their ability to support intrafilm acidification and detritylation, eleven deficient in electronegative heteroatoms supported detritylation and intrafilm acidification to no less an extent than a film of **2** without polymer. A further six either lacking heteroatoms, or containing aryl halides or a trisilane group, gave more moderate support. The remaining 26 were polymers of subunits containing electronegative heteroatoms (O, N, Cl): they supported acidification and detritylation only poorly or not at all (ESI†).

Hydrogen bonding by photoacid generators. PMMA and other oxygen-containing polymers weakened intrafilm TCA strength, whereas compounds **1–10** and **20–25** did not, despite their high oxygen contents. This difference between oxygen-containing polymers and PAGs can be rationalised by reference to the detailed studies of Laurence *et al.*[21] on H-bonding strengths. They point to the following conclusions: (a) the strongest H-bonding group of

1–10, **20–25** and **29** is the ester carbonyl, (b) TCA esters have lowered H-bonding because of the strong electron withdrawing effect of the trichloromethyl group (c) the 2-nitro group is a modest H-bonder.

Loss of the H-bonding ester group on photolysis and concomitant conversion of 2-nitro to a 2-nitroso group with possibly weaker H-bonding may explain the sigmoid relation between photoacid concentration and extent of detritylation (Fig. 6). Variations of H-bonding may underlie the varying ability of PAGs, although lacking nitrogenous substitutions as in **11–19**, to effect the same extent of detritylation for the same extent of photolysis. Thus **2** is more effective than **1** but less effective than **7**.

Kinetics of detritylation

Fig. 5 shows detritylation kinetics for a film of polymer and **2** (8 : 1, w/w) containing DMT-T during continuous or interrupted illumination at 365 nm. In the main part of Fig. 5, DMT^+ production rapidly reached a plateau despite continuing photolysis. The brief lag phase at the onset of illumination is a constant feature of these experiments. The insert graph shows that detritylation in response to interrupted illumination stopped promptly within 5–10 s of the end of each illumination period. Similar behaviour was observed with other heteroatom-deficient polymers and various ratios of polymer to ester **2**.

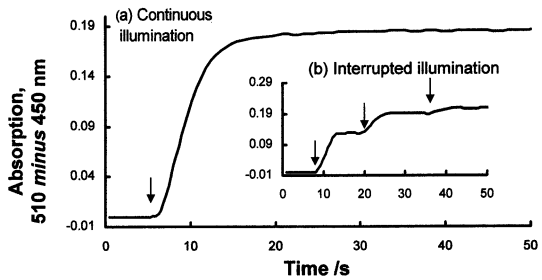

Fig. 5 Kinetics of detritylation. Films cast from a solution of PMS (2% w/v), ester **2** (0.25% w/v), 0.2 mM DMT-T. Appearance of DMT^+ in films measured in dual wavelength mode at 510–550 nm. The larger recording (a) is for continuous 365 nm illumination (13 mW cm^{-2}) starting at the arrow. The smaller panel (b) is for 3 separate illumination periods of 5 s each, again at 13 mW cm^{-2} and commencing at the arrows.

Equilibrium constant for detritylation

An apparent equilibrium constant for acid-induced detritylation of DMT-T can be defined as:

$$K_{eq} = \frac{[\text{T-OH}][\text{DMT}^+\text{A}^-]}{[\text{DMT-T}][\text{HA}]} \quad (1)$$

where DMT^+A^- is the ion pair anticipated in an aprotic medium and DMT-T is 5′-*O*-dimethoxytritylthymidine. [HA] is the total concentration of a protic acid and includes both undissociated acid and the ion pair H^+A^-. K_{eq} is dimensionless, and when all reaction participants are dispersed throughout the same film volume, concentrations can be replaced with area densities. Use of [HA] rather than $[H^+]$ in eqn (1) makes K_{eq} dependent on the pK_a of the acid.

Data for calculation of K_{eq} were obtained in experiments as in Fig. 6, where repeated brief illuminations of a film of ester

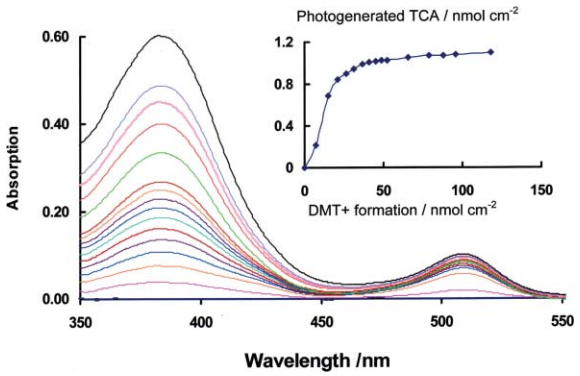

Fig. 6 Stepwise detritylation. The larger graph has a set of spectra from a film, 1.5 μm thick, cast from 1% PMS (w/v), 1% ester **2** (6.3 mM) and DMT-T (0.3 mM) in DCM, and exposed to 13 mW cm^{-2} at 365 nm for 10 successive exposures of 5 s each followed by 4 at 20 s each and finally 1 at 80 s. A spectrum was recorded 10 s after each exposure: their positions in the graph are in ascending duration of cumulative exposure. All spectra were referenced to the pre-photolysis spectrum to give difference spectra and a flat zero-time baseline. The emergent peak at 384 nm is due to nitroso-photoproduct accumulation. The smaller graph is a plot of the area density of DMT^+, calculated from the peak at 510 nm, against TCA area density. The latter was derived from the assumption that the area density of TCA is equal to that of the substituted 2-nitrosobenzophenone as calculated from the light-induced absorption peak at 384 nm.

2 containing DMT-T resulted in photoacid accumulation and detritylation. The increments of DMT^+ release became smaller with increasing number of illumination periods, finally becoming almost undetectable even though further photoacid was generated. This behaviour is that of a system being repeatedly progressed from one equilibrium position to the next, towards but never achieving complete detritylation.

The relationship between the area densities of photoacid and DMT^+ is shown as an insert within Fig. 6. Release of DMT^+ commenced after a brief lag-phase, and proceeded with increasing photoacid generation to a plateau that did not entirely flatten. Part, at least, of the continuing but small increase at 510 nm was due to a contribution from the long-wavelength absorption tail of the nitroso-photoproduct. The extent of detritylation in the plateau region was 80–90%.

K_{eq} as defined in eqn (1) is dimensionless, and area densities can be used for its calculation in place of concentrations. The calculated values for several experiments lay between 0.02 and 0.1. We ignored the lag in DMT^+ formation following commencement of illumination, so our calculated values are underestimates. Because total acid concentration is used in place of proton activity, the effect of acid strength is buried within the value of K_{eq}, which is therefore specific to a given photoacid.

Inhomogeneous distribution of photoacid generator and DMT-T in films composed of both polymer and photoacid generator would create photoacid-deficient microdomains of DMT-T resulting in an equilibrium position that was lowered due to failure of photoacid to contact all DMT-T molecules, unless inter-domain diffusion equilibrated concentrations. We have not observed significant differences between the apparent equilibrium constants for films of photoacid generator with or without added polymer. So if microdomains did exist, either their effect was negated by diffusion or contributed too little to be detected in these

experiments where the intrafilm diffusion coefficient for TCA was sufficiently high (50 nm^{-2} s^{-1})[22] to allow movement over several hundred nm during the experiment.

Esters of other acids as photoacid generators

Photolysis of **26** releases *p*-toluenesulfonic acid. The quantum yield in solution was low, *ca.* 0.02, rising to 0.06 in films of PMS or PSMS. The extent of photolysis required to cause comparable detritylation of intrafilm DMT-T was lower than that required by photolysis of **2**, in keeping with the greater strength of *p*-toluenesulfonic acid. Photolysis of **26** in films of PMMA compared to PSMS was not inhibited, but a three-fold increase of intrafilm acid concentration was required to obtain comparable detritylation of intrafilm DMT-T. Thus the effects of electronegative atoms in a polymer apply to *p*-toluenesulfonic acid, although less severely than they do to TCA.

Ester **28** releases HBr on photolysis, and although lacking an α-phenyl group, it performed similarly to **2** when tested for detritylation in films of PS. The HCl-releasing **27** was less effective, suffering from low light absorption at 365 nm. Ester **29** is a photogenerator for acetic acid, which was several-fold less effective at detritylation than comparable intrafilm concentrations of TCA. None of these alternative acids appeared to offer any advantages over TCA.

Design of TCA photogenerators based on substituted 2-nitrobenzylalcohols

Electron withdrawing substitutions of the 2-nitrobenzyl ring such as halides or NO_2 groups typically increase the quantum yield and lower both the height and wavelength of the absorption maximum, whereas amino groups have the opposite effects. The quantum yield enhancing effects of α-methyl or α-phenyl substitution are well known, as is the similar effect of a second nitro-group at the 6-position. That leaves positions 3–5 for substitutions that may shift absorption bands from >300 nm to higher wavelengths. Several useful 4- and 5-substituted 2,6-dinitrobenzyl esters of TCA, all α-phenyl substituted, were identified (**2**, **7**, **21–24**). Esters **24** and **28** were the only 2,6-dinitrobenzyl esters not substituted at either the 3- or 5- position. Comparison of the isomeric pair **22** ($\Phi \approx 0.3$) and **24** ($\Phi \approx 0.8$) shows that substitution at the 4-position to create a symmetrically substituted 2-nitrobenzyl ring favours a high quantum yield.

A further consideration is that neither the ester nor its photoproduct should bind protons at the intrafilm proton activity required for extensive detritylation. For this reason, the alkyl- and aryl-amino substituted esters **11–18** were ineffective, despite excellent absorption properties and an adequate quantum yield in **15**. The remaining ester of this class, **19**, had a quantum yield too low to be useful. But the substituted 2-nitrobenzyl alcohol precursor of ester **15** might be useful as a starting point for a protecting group for other applications (*e.g.* photogenerators of bases).[23]

Polymer matrices. Previous reports[9] of photoacid generation in diffusion-restricting solid films as part of the fabrication of oligonucleotide arrays described mainly PMMA as a film forming support polymer for the PAG.

We found that PMMA and numerous other polymers containing electronegative heteroatoms weaken TCA at ambient temperature (Fig. 3 and 4, and ESI†). A similar phenomenon also attributed to hydrogen bonding has been reported between dichloroacetic acid and the solvent acetonitrile when used for detritylation in solid-phase oligonucleotide synthesis.[24] We identified several polymers that are suitable as inert matrices for photogenerated TCA. Examples are polystyrene, poly(α-methylstyrene, poly(styrene-*co*-α-methylstyrene), polylimonene and poly-(indene-*co*-coumarone). The last of these contains oxygen but the content is low, < 2% by wt, and does not have a significant effect on TCA strength (Supporting Information).

The acidic hydrogen of other acids can also participate in hydrogen bonds. We observed partial inhibition by PMMA, but not PSMS, of the ability of photogenerated *p*-toluenesulfonic acid to effect intra-film detritylation. Heteroatom-deficient polymers may therefore be the preferred matrix for other photoacids such as alkyl- or aryl-sulfonic acids.

Not all photoacid generators can themselves form films when cast from solution but even when they do, as with most of those described in Table 1, there are advantages in using a polymer matrix: *e.g.* control of the concentration of PAG and intrafilm viscosity. On the other hand a film composed solely of PAG cannot form PAG-deficient microdomains.

Photoacid performance in solid films. The detritylation target in our experiments was DMT-T incorporated within diffusion-restricting solid films. Detritylation is reversible, and its equilibration following photoacid generation was attained within *ca.* 10 s. The apparent K_{eq} value using ester **2** in a PMS film was *ca.* 0.02–0.1, and even at intrafilm TCA concentrations of 1.9 M, the extent of detritylation did not exceed 80–90%.

The relation between photoacid concentration and extent of detritylation at equilibrium for a given value for K_{eq} and initial DMT-T concentration can be calculated, with results as in Fig. 7. The important conclusion is that the approach of detritylation towards completion is asymptotic, becoming highly insensitive to increasing acidity once detritylation reaches *ca.* 96%. Unless photoacid is at least 50-fold stronger than TCA, the achievable photoacid level in a film would be unable to achieve >99%

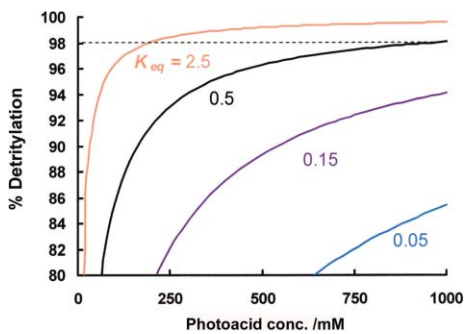

Fig. 7 Effects of photoacid concentration and K_{eq} on extent of detritylation at equilibrium. Eqn (1) was rearranged to yield [HO-oligonucleotide] as the variable in a quadratic equation which was then solved for a range of HA concentrations for given values of initial DMT-T concentration and K_{eq}. The plots are for calculated % detritylation in response to varied concentration of HA over a range of K_{eq} values from 0.05 to 2.5. The initial value for DMT-O-oligonucleotide concentration was 10 mM.

completion of detritylation (Fig. 7, compare $K_{eq} = 2.5$ with $K_{eq} = 0.05$).

Experimentally determined detritylation also showed asymptotic behaviour as it reached higher levels in response to increasing photoacid concentrations (Fig. 6).

Conclusions

We have provided effective photogenerators of TCA based on esters of substituted 2-nitrobenzyl alcohols. They form solid, uniform and optically clear films without addition of polymers. The presence of electronegative heteroatoms in polymers when included in the films renders TCA ineffective as a DMT-T detritylation agent. Equilibrium of detritylation reactants is reached within 5–10 s. Both experiments and simulations show that higher levels of detritylation are approached only asymptotically. Pushing the reaction towards completion with strong acids or high concentrations is an unsatisfactory approach. Future emphasis should be on removal of DMT^+ despite the presence of solid films.

Experimental

Synthesis of photoacid generators

Esters **1–25** described in the results section table are based on α-phenyl-2-nitrobenzylalcohol. Full synthetic details and spectroscopic characterisation of the esters and examples of nitroso-photoproducts are given in the ESI.† We have previously described[11] the synthesis of esters **1** and **2**.

Thin solid films on glass of esters or esters with polymer

We used glass microscope slides, either intact or cut down to *ca.* 25 × 6 mm slices. Film-casting solutions, typically 0.5–2% (w/v) in DCM, were used in one of two ways: either dip-coating or spreading. Dip-coating makes more uniform films, on both sides of a slide. Unwanted film on one side can be removed with tissue moistened with solvent. Alternatively, the two films can remain and both are photolysed and measured together in series, doubling the measured absorption changes. Another alternative is to first coat one side of the slide with an anti-wetting agent (Repelcote, a 2% v/v solution of dimethyldichloro-silane in octamethylcyclotetrasiloxane, from Merck Ltd, Poole, Dorset, UK). The thickness achieved by dip-coating was varied by changing the concentration of the casting solution, or varying the speed at which the slide was withdrawn from the solution.

Spreading used glass diagnostic slides, 75 × 25 × 1 mm (VWR International, Lutterworth, Leicestershire, UK, or www.vwr.com) that carry on one face a hydrophobic mask of black Teflon that exposes one or more circular areas of the glass surface, each typically 10–15 mm in diameter. These areas form shallow wells, and 10–15 μL of casting solution placed with a micro-syringe into one of them on a horizontal slide rapidly spreads over the exposed glass area and evaporates to leave a circular film. If wished, pre-heating of the slide to 45–55 °C accelerates drying, and protects the film area against evaporative cooling that could attract water condensation from the atmosphere.

Apparatus for photolysis and spectrophotometry of thin films on glass slides

This laboratory-constructed instrument is described in the ESI.† Sensitivity varied with the detector, but for the experiments described here, sensitivity was not an issue because DMT-T was present throughout the films to give area densities several-fold higher than those obtainable by its attachment as a monolayer to the underlying glass.

Measurement of proton activity in films

We used a pH indicator in the casting solutions to yield films incorporating a spectrophotometric measure for intra-film proton activity. Amongst a variety of pH indicators[18] with solution pK_a values around 0.5–1.0, the triphenylmethane cationic indicator brilliant green was the most suitable. It dissolves in DCM, where it has a pH-sensitive absorption peak at 630 nm ($E_{mM} = 96\ mM^{-1}\ cm^{-1}$), and relatively low absorption in the green–blue–UV spectral region. Other indicators with higher pK_a values and suitably placed absorption bands can be used in combination with BG to extend the response range to include weaker acids. The absorption spectrum of BG responded predictably to changes of photoacid acid concentration in solid films.

Measurement of photoacid acid production in films

Photolysis of substituted 2-nitrobenzyl esters produces the corresponding acid and substituted 2-nitrosobenzophenones. Alternative reaction routes are negligible, and there is a 1 : 1 stoichiometry between acid release and formation of the 2-nitrosobenzophenone photo-product. The absorption difference spectrum of *after* minus *before* photolysis is due to generation of the 2-nitrosobenzophenone, as shown in Fig. 6. The area density of the 2-nitrosobenzophenone photoproduct can be calculated from the peak height, and is assumed to equal that of photogenerated acid. For ester **2**, the difference spectrum between *after* and *before* photolysis has a peak at 384 nm, with $\varepsilon_{mM} = 4.1\ mM^{-1}\ cm.^{-1}$

Detritylation of intrafilm DMT-T

Measurement of the extent of detritylation requires that the value of pre-photolysis intrafilm DMT-T density is known. To obtain this value, we first measured in a sample of the film casting solution, diluted 100–200 fold in 2.5 ml DCM, the value of the 324 nm shoulder due to the presence of ester **2**. Addition of 2 M TCA to obtain a final concentration of 0.05 M gave a 505 nm peak due to essentially complete conversion of DMT-T to DMT^+. The ratio of the two peak heights was used as a factor to convert the 324 nm reading in films to the anticipated 510 nm peak if all DMT-T were to be detritylated. The observed 510 nm reading in response to photolysis was then used to calculate the extent of DMT-T detritylation.

Measurement of film thickness

At the onset of this work, we made measurements by interferometry, using the spectrophotometer with a reflectance probe. The intensity of reflected light as a function of wavelength was measured over the range from 400 or 450 nm to 870 nm. Peaks and troughs were observed, their number increasing with film

thickness. A glass slide without a film was used as the reference. For calculation of film thickness, we used a model with normal incidence of the light beam on the film, and interference between the back reflections from the first and second interfaces, namely air/film and film/glass. The effects of multiple reflections are negligible and can be ignored. But otherwise we obtained the film thickness from the absorption spectra. The area density (nmol cm^{-2}) of PAG was calculated from the characteristic pre-photolysis UV-absorption of the PAG, using ε_{mM} values from Table 1. The area density of material (μg cm^{-2}) was then calculated from the PAG density (and the casting solution composition if polymer was also included), and converted to a film thickness on the assumption that the film density was 1 g cm^{-3}.

Acknowledgements

This work was supported by The Institute for Cancer Research and grant no. EGM/16064 provided jointly by the Biotechnology and Biological Sciences Research Council (BBSRC) and the Engineering and Physical Sciences Research Council (EPSRC). Early stages of the work were assisted by an Emeritus Fellowship to PBG from the Wolfson Foundation. We are indebted to Dr Amin Mirza for performing MS analyses and to Professor Colin Cooper for his support and encouragement.

References

1 P. J. Kocieński, *Protecting Groups*, Georg Thieme Verlag, Stuttgart, 2nd edn, 2000, pp. 269–274.
2 Abbreviations: A^- and HA, acid anion and acid respectively; BG, brilliant green; DCM, dichloromethane; DMT, 4,4′-dimethoxytrityl group; DMT^+, 4,4′-dimethoxytrityl cation; DMT-T, 5′-*O*-dimethoxytritylthymidine; ester **1**, trichloroacetate ester of α-phenyl-4,5-dimethoxy-2-nitrobenzyl alcohol; ester **1** photoproduct, 4,5-dimethoxy-2-nitrosobenzophenone; ester **2**, trichloroacetate ester of α-phenyl-4,5-dimethoxy-2,6-dinitrobenzyl alcohol; ester **2** photoproduct, 4,5-dimethoxy-6-nitro-2-nitrosobenzophenone; PAA, 4-phenylazoaniline; PAG, photoacid generator; PMMA, poly(methylmethacrylate); PMS, poly(α-methyl-styrene); PS, polystyrene; PSMS, poly(styrene-*co*-α-methyl-styrene); TCA, trichloroacetic acid.
3 M. Smith, D. H. Rammler, I. H. Goldberg and H. G. Khorana, *J. Am. Chem. Soc.*, 1962, **84**, 430–440.
4 S. L. Beaucage and R. P. Iyer, *Tetrahedron*, 1992, **48**, 2223–2311.
5 M. H. Caruthers, *Acc. Chem. Res.*, 1991, **24**, 278–284.
6 S. P. A. Fodor, L. J. Read, M. C. Pirrung, L. Stryer, A. T. Lu and D. Solas, *Science*, 1991, **251**, 773–776.
7 X. Gao, P. Yu, E. LeProust, L. Sonigo, J. P. Pellois and H. J. Zhang, *J. Am. Chem. Soc.*, 1998, 12698–12699; X. Gao, E. LeProust, H. Zhang, O. Srivannavit, E. Gulari, P. Yu, C. Nishiguchi, Q. Xiang and X. Zhou, *Nucleic Acids Res.*, 2001, **29**, 4744–4750.
8 X. Zhou, S. Cai, A. Hong, Q. You, P. Yu, N. Sheng, O. Srivannavit, S. Muranjan, J. M. Rouillard, Y. Xia, X. Zhang, Q. Xiang, R. Ganesh, Q. Zhu, A. Matejko, E. Gulari and X. Gao, *Nucleic Acids Res.*, 2004, **32**, 5409–5417.
9 G. Wallraff, J. Labadie, P. Brock, R. DiPietro, T. Nyugen, T. Huynh, W. Hinsberg and G. McGall, *CHEMTECH*, 1997, 22–32; J. E. Beecher, G. H. McGall and M. J. Goldberg, *Polym. Mater. Sci. Eng.*, 1997, **76**, 597–598; J. E. Beecher, M. J. Goldberg, G. H. McGall, US Pat., 6 083 697, 2000; M. J. Goldberg, R. G. Kulmeilis, G. H. McGall, N. A. Parker, G. Xu, US Pat. Appl. 0 164 258 A, 2005.
10 A. B. Sierzchala, D. J. Dellinger, J. R. Betley, T. K. Wyrzykiewicz, C. M. Yamada and M. H. Caruthers, *J. Am. Chem. Soc.*, 2005, **125**, 13427–13441.
11 P. J. Serafinowski and P. B. Garland, *J. Am. Chem. Soc.*, 2003, **125**, 962–966.
12 F. M. Houhilan, T. X. Neenan, E. Reichmanis, J. M. Kometani and T. Chin, *Chem. Mater.*, 1991, **3**, 462–471.
13 E. Reichmanis, B. C. Smith and R. Gooden, *J. Polym. Sci., Polym. Chem. Ed.*, 1985, **23**, 1–8.
14 T. X. Neenan, F. M. Houlihan, E. Reichmanis, J. M. Kometani, B. J. Bachman and L. F. Thompson, *Macromolecules*, 1990, **23**, 145–150.
15 Referred to as esters A and D rather than **1** and **2** in P. J. Serafinowski and P. B. Garland, *J. Am. Chem. Soc.*, 2003, **125**, 962–965.
16 M. Irie, Y. Hirano, S. Hashimoto and K. Hayashi, *Macromolecules*, 1981, **14**, 262–267.
17 H. Barzynski and D. Sanger, *Angew. Makromol. Chem.*, 1981, **93**, 131–141.
18 F. J. Green, *The Sigma-Aldrich Handbook of Stains, Dyes and Indicators*, Aldrich Chemical Company Inc., Milwaukee, USA, 2nd edn, 1991.
19 J. D. Roberts and M. C. Caserio, *Basic Principles of Organic Chemistry*, W. A. Benjamin Inc., London, 2nd edn, 1977, pp. 791–793.
20 R. L. Miller, in *Polymer Handbook*, ed. J. Branderup, E.H. Immergut and E. A. Grulke, J. Wiley & Sons Inc., Chichester, U.K., 4th edn, 1999, pp. V1/113-VI/124; Aldrich Polymer Products CD-Catalogue and Reference Guide, 2000, available at www.sigmaaldrich.com.
21 C. Laurence, M. Berthelot, M. Lucon and D. G. Morris, *J. Chem. Soc., Perkin Trans. 2*, 1994, 491–493; C. Laurence, M. Berthelot, M. Herbert and K. Sraïdi, *J. Phys. Chem.*, 1989, **93**, 3799–3802; F. Besseau, C. Laurence and M. J. Berthelot, *J. Chem. Soc., Perkin Trans. 2*, 1994, 485–489.
22 P. B. Garland and P. J. Serafinowski, unpublished work.
23 J. F. Cameron and J. F. Fréchet, *J. Am. Chem. Soc.*, 1991, **113**, 4303–4313.
24 C. H. Paul and A. T. Royappa, *Nucleic Acids Res.*, 1996, **24**, 3048–3052.